Am J Cancer Res 2023;13(4):1278-1294
www.ajcr.us /ISSN:2156-6976/ajcr0147609

Original Article

The signature of immune-subtype specific driving transcription factors suggest potential drugs for refractory glioblastoma

Wenjin Chen[1,2*], Lihua Chen[2*], Lili Guo[2], Ning Liu[3], Tao Wu[1], Yajing Cheng[4], Pengfei Xu[1], Yifei Li[1], Xiaofang Yang[1], Ruxiang Xu[2], Baodong Chen[1]

[1]Department of Neurosurgery, Peking University Shenzhen Hospital, Shenzhen Peking University-The Hong Kong University of Science and Technology Medical Center, Shenzhen 518000, Guangdong, P. R. China; [2]Department of Neurosurgery, Sichuan Academy of Medical Science and Sichuan Provincial People's Hospital, University of Electronic Science and Technology of China, Chengdu 610072, Sichuan, P. R. China; [3]Department of Neurosurgery, The Seventh Medical Center of PLA General Hospital, Beijing 100000, P. R. China; [4]Department of Neurology, Peking University Shenzhen Hospital, Shenzhen Peking University-The Hong Kong University of Science and Technology Medical Center, Shenzhen 518000, Guangdong, P. R. China. [*]Equal contributors.

Received November 8, 2022; Accepted March 31, 2023; Epub April 15, 2023; Published April 30, 2023

Abstract: Immunocharacteristics-based typing strategies can be used to reflect the similar status of tumors. Therefore, we aimed to demonstrate whether the immune subtypes of GBM have independent prognostic efficacy and whether these subtypes can be used as clinical guidance for predicting the progression of GBM and determining drug sensitivity. In this study, we found that patients with GBM were divided into three conserved immune-related subtypes based on the infiltration level of immune cells, including immunosuppressed, moderate immunoactivity, and high immunoactivity. Regarding the relevant clinical significance, the high immunoactivity in GBM indicates the worst survival, which exhibited the highest levels of oncogenic activity, including angiogenesis, tumor-associated macrophages and tumor-associated fibroblasts, indicated worst survival. The immunosuppressive subtype of GBM was more likely to carry epidermal growth factor receptor mutations and MGMT methylation, and belong to the classical and proneural subtypes; however, but the high immunoactivity subtype was not. The immune subtype-specific transcription factors (TFs) regulatory network indicates that specific TFs drive the construction of each immune subtype, and that these subtype-specific TFs are more prone to internal TFs regulation. Furthermore, the immunosuppressed and moderate immunoactivity subtypes were significantly correlated with the drugs sensitivity, whereas the high immunoactivity subtype was not, indicating that GBMs with high immunoactivity were refractory. We also found that obatoclax mesylate, NPK76-II-72-1, gemcitabine, TAK-715 are potential drugs for the treatment of refractory GBM based on drug sensitivity models of different immune subtypes. Therefore, we demonstrated that the immune subtypes of GBM have independent prognostic efficacy and can be used as clinical guidance for predicting the progression of GBM and drug sensitivity. Most importantly, this study is expected to provide a pathway for the development of effective drugs for treatment of refractory GBM.

Keywords: Glioblastoma, immune infiltration, immune subtypes, transcription factors, drug sensitivity

Introduction

Glioblastoma multiforme (GBM) is the most common primary malignant brain tumor, which accounts for approximately 57% of all gliomas [1, 2]. Since GBM is highly susceptible to recurrence after the maximal safe surgical resection, can develop resistance to the conventional fractionated radiotherapy and standard temozolomide chemotherapy, and exhibits an extremely poor clinical prognosis [3, 4]. Cancer immunotherapy is a newly advanced therapy that results in effective clinical outcomes by achieving long-lasting tumor remission in many defined cancer types [5]. However, many studies have shown that immunotherapy has a great difference in the therapeutic effects on the same cancer, especially in GBM [6, 7]. Monoclonal antibodies against PD-1, PD-L1 and CTLA-4 have been used in clinical trials. A

Phase III trial showed that nivolumab, a monoclonal antibody against PD-1, did not prolong the median overall survival in recurrent GBM compared with bevacizumab [8]. Nivolumab in combination with ipilimumab, a monoclonal antibody against CTLA-4, did not significantly improve the clinical outcome as well [9]. Two other retrospective studies revealed that anti-PD-1 salvage therapy did not provide survival benefits to patients with recurrent high-grade gliomas [10, 11]. Thus, understanding why GBM outcomes differ among patients receiving the same treatment, especially the underlying mechanism, is the cornerstone of a more comprehensive approach to improve diagnostic accuracy and individualized treatments.

In this study, we analyzed the correlation between the immune microenvironment of GBM and drug sensitivity. Patients with GBM were clustered into three conserved immune-related subtypes based on the level of immune cells infiltration: immunosuppressed, moderate immunoactivity, and high immunoactivity. We found that these immune-related subtypes could predicts the survival status with higher levels of immune infiltration, higher protumor activity, and worse overall survival (OS) and the progression free survival (PFS). For the underlying mechanism, we found that specific transcription factors (TFs) drive the formation of different immune subtypes in GBM, and there is a significant relationship between immune subtype-specific TFs and anti-tumor drug sensitivity. TFs that drive high immunoactivity tend to exhibit poor drug sensitivity. However, there was a high level of anti-tumor drug sensitivity in the driving TFs of the other two immune subtypes. Therefore, this study is the first to reveal that there are three conserved immune-related subtypes in GBM, and that the immune infiltration status could predict clinical prognosis. Most importantly, we were the first to identify the relationship between the specific immune-related subtype driving TFs and the sensitivity of anti-tumor drugs. Most importantly, we believe that these findings may provide important scientific clues for GBM treatment in the future studies.

Materials and methods

Databases and preprocessing

The Cancer Genome Atlas (TCGA) GBM (TCGA-GBM) genome transcriptome data (RNA-seq), genome mutation data (WES) and the related clinical information obtained from 153 patients with GBM, were downloaded from the cBioPortal database (https://www.cbioportal.org/) and used as the analysis set. RNA-seq data included the count and Fragments Per Kilobase of transcript per Million mapped reads (FPKM) expression profiles [12]. For genome mutation data, silent mutations were removed by preprocessing. The FPKM expression spectrum was log-processed (log2FPKM). Survival data, OS, PFS, and clinical phenotype data (including age, sex, and whether radiotherapy had been received) of patients with GBM, and the expression subtype, MGMT methylation status, and IDH1/TP53/EGFR mutation status of GBM samples, were also downloaded. A dataset that included the clinical information and transcriptome data (GSE4412) of 85 patients was downloaded from the Gene Expression Omnibus (GEO) resources platform (https://www.ncbi.nlm.nih.gov/gds) and used as the validation set [13].

Construction of immune subtypes in GBM

We obtained 22 gene sets of immune cell types based on previous human studies and 29 gene sets of tumor microenvironment characteristics (TME 29 FGEs) based on previous studies, including 20 immune cell characteristics and nine cancer-promoting characteristics based on mRNA expression levels (log2FPKM) of the related immune cells in these GBM samples [14-16]; The infiltration level (also called immunoactivity) and oncogenic characteristic activity of these immune cells in these samples were calculated using the single-sample Gene Set Enrichment Analysis (ssGSEA) method. In addition, we calculated the infiltration level of immune cells according to the MCP-counter and Timer2.0 methods [17, 18]. For TCGA-GBM analysis and GSE4412 GBM independent validation set samples, the unsupervised hierarchical clustering method was used to perform cluster analysis on GBM samples according to 22 immune cell infiltration levels, and the optimal cluster number of samples was determined using inflection point method.

Evaluation of the characteristic of TMZ among immune subtype-specific GBM

To evaluate the FPKM expression profile data, the R package ESTIMATE was used to calculate

the immune and stromal scores based on the proportion of stromal and immune cells [19]. The CYT activity score was calculated using the mean of GZMA and PRF1 gene expression (log2FPKM) [20, 21]. The IFN-γ pathway and its genes were collected from the Molecular Signature Database (V7.4), and the activity score of IFN-γ pathway was calculated using the ssGSEA method. Two tumor-promoting features, angiogenesis and cancer-associated fibroblasts, were isolated from the TME 29 FGES. Statistical tests were used to explore differences in these characteristics between immune subtypes: the Kruskal_Wallis test was used for significance analysis between multiple groups, and the Wilcoxon rank sum test was used for significance analysis between two groups. We used the expression levels of the samples (log2FPKM) to conduct a classification analysis of GBM samples using the Louvain community classification method and then mapped the immune subtypes into the Louvain community classification [16]. By extracting the activity levels of some tumor microenvironment features (including natural killer cells, oncogenic features, and angiogenesis), their distributions in different sample subtypes were characterized. In addition, we used heat maps to show the activity levels of nine oncogenic features in the TME and their distribution in different immune subtypes.

Comparison of clinical features and prognostic efficacy among immune subtype-specific GBM

Based on the immune subtypes of GBM samples, we used the log-rank test to explore the differences in survival time, including OS and PFS, among immune subtypes, and then used the R-package survival to draw Kaplan-Meier curves of the patients with different subtypes. Univariate Cox regression analysis was used to characterize the prognostic efficacy of immune subtypes. Clinical characteristics (including age, sex, and whether radiotherapy has been received), the distribution of expression subtypes, MGMT methylation status, and IDH1/TP53/EGFR mutation status in different subtypes were explored. Multivariate Cox regression analysis was used to explore whether the immune subtypes were independent of other clinical variables.

Analysis of functional enrichment among immune subtype-specific GBM

DESeq2 based on gene expression level (count), and differential expression genes between subtypes were screened based on thresholds (FC ≥1.5 or FC ≤2/3, FDR ≤0.05, Benjamini & Hochberg corrected significance level). The differentially expressed genes of all subtypes were extracted from the samples compared with other samples, and those of the GBM immune subtypes were obtained through intersection processing. Subsequently, these differentially expressed genes were analyzed for gene ontology (GO) functional enrichment (BP, CC, and MF) and KEGG pathway enrichment using the R-packet ClusterProfiler. The top15 GO terms and top 20 enrichment pathways were screened out and displayed according to the significance level.

Construction of immune subtype-specific TFs regulatory network

The GBM regulator was downloaded from Viper (http://califano.c2b2.columbia.edu/viper). The master regulator of each immune subtype was identified according to the genome expression level of GBM samples (log2FPKM) based on the Viper algorithm (each subtype was compared with all other subtypes) [22], and TFs specific to the immune subtype were extracted. Finally, we calculated the mutual information between TFs using the R package (MINET). In general, the correlation number reflects the linear correlation between variables, whereas mutual information directly considers the mutual independence between variables from the perspective of the probability distribution. Mutual independence is not necessarily correlated and non-correlation is not necessarily independent. Using the mutual information method can eliminate information loss caused by correlation. Therefore, a regulatory network between TFs was constructed according to the mutual information between TFs (weight > 0.1).

Drug sensitivity analysis based on immune subtypes

We expressed data from the Genomic of Drug Sensitivity in Cancer (GDSC) database (https://www.cancerrxgene.org/), cell lines (array data), drug response information (logIC50), and joint TCGA-GBM sample expression spectrum (FPKM), using the R package to eliminate the sva batch effect. Combined with this information, a ridge regression model was constructed using the Ridge package to predict drug sensitivity in patients within the TCGA-GBM dataset [23]. During processing, more than 10 drug sample with values of 0 were removed. Spearman's

rank correlation was calculated according to the expression levels of TFs specific for each immune subtype in the GBM samples (log2FPKM). We selected each specific immune subtype TF according to the correlation coefficient of |R| > = 0.2 and significant P.adj < = 0.01 and the relationship between drugs on. To characterize the specificity of drug-related TFs of each immune subtype, we required that the number of TFs related to a certain drug in the same subtype should exceed 60% of the number of TFs specific to all subtypes, and then determine the relationship between TFs and drugs for subsequent analysis. Information on the interactions between drugs targets and pathways was downloaded from the GDSC database. By calculating the Pearson correlation between the expression level of immune subtype-specific TFs and the expression level of corresponding drug targets, significant TFs and target pairs were selected, and a network diagram of the TFs-drug-target-pathway was drawn using Cytoscape (V3.5.0) software combined with drug and pathway information.

Statistical analysis

GraphPad Prism 8 (GraphPad Software Inc., USA) was used to perform the statistical analyses and chart making. All statistical analyses were performed using R statistical language (version 4.0.5). Wilcoxon and Kruskal-Wallis tests was used for the significance comparison between two groups and multiple groups, respectively. The Kaplan-Meier plotter was used to draw the prognostic survival curve, and the log-rank test was used to evaluate the significance of the statistical difference. Spearman's test was used for correlation analysis and calculation of correlation coefficient. All survivorship curves were generated using R package. The OS and risk scores were calculated using the R package survival and cutoff values determined. Based on the dichotomized risk scores, patients were grouped into high or low risk score in each data set, and the computational batch effect was reduced by the R package sva. In all analyses, each group of experiments was repeated at least three times, standard deviation (SD) was calculated to indicate the variation within each experiment and data, and values represent mean ± SD. $P < 0.05$ was considered statistically significant.

Results

Immune subtypes of GBM and their oncogenic features

Subgroup analysis can be used to reflect the similar state of tumors, thus, helping personalize treatment. In this study, we analyzed the level of immune infiltration in GBM samples and constructed a cluster spectrum. Briefly, 22 immune cell-specific marker gene sets were obtained based on previous studies, and the infiltration level of immune cells was calculated using the ssGSEA method. The 153 TCGA-GBM samples were then divided into three classes (immune subtypes) using unsupervised hierarchical clustering based on the level of immune cell infiltration. Cluster 1 was characterized by immunosuppression and included 58 cases; Cluster 2 was characterized by moderate immunoactivity and included 58 cases; and Cluster 3 was characterized by high immunoactivity and included 17 cases (**Figure 1A**, top panel). In addition, we used the McP-counter and Timer2.0 methods to calculate the infiltration level of immune cells in these GBM samples, and found that consistent classes were constructed compared to hierarchical clustering (**Figure 1**, middle and below panel).

To explore the oncogenic features of different immune subtypes in GBM, we firstly performed a survival analysis on these identified immune subtypes. We found significant differences in OS and PFS among different immune subtypes in patients with GBM, which were characterized by the worst OS and PFS in Cluster 3, indicating that high immunoactivity in GBM predicts poor clinical prognosis (**Figure 1B**). To explain this phenomenon, we obtained nine cancer-promoting signatures of TMEs from previous studies, including angiogenesis, endothelium, matrix remodeling, cancer-associated fibroblasts, matrix, neutrophil signature, tumor-associated macrophages, protumor cytokines, and granulocyte traffic. Oncogenic activity was calculated using the ssGSEA method, and we found that patients in Cluster 3, who exhibited shorter survival time, showed stronger oncogenic characteristics, whereas patients in Cluster 1 who exhibited longer survival time, showed inhibition of oncogenic characteristics (**Figure 1C**).

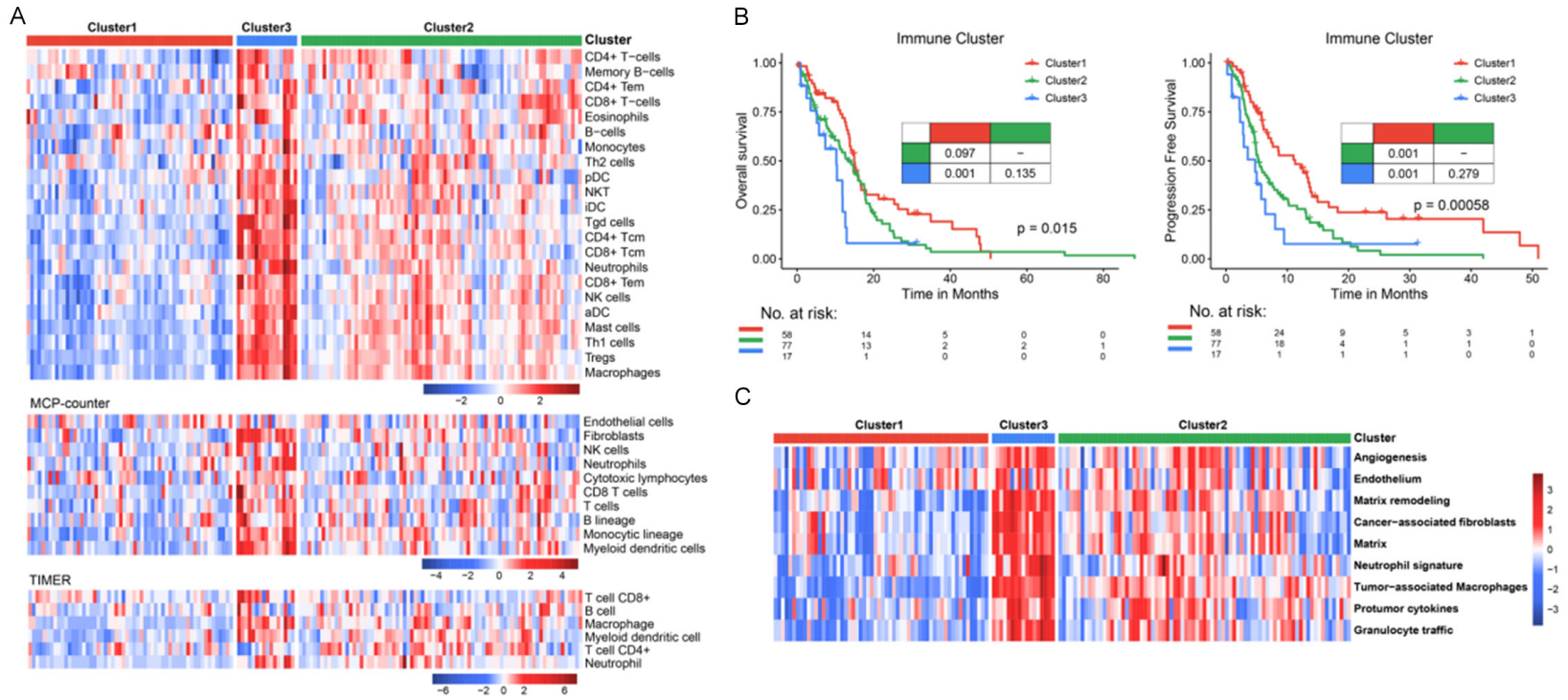

Figure 1. Unsupervised hierarchical cluster analysis based on immune activity levels in TCGA-GBM samples and the clinical relevance analysis. A. Heat map of the immune activity levels calculated using the single-sample GSEA (ssGSEA) method, MCP-counter, and Timer2.0 methods. B. GBM sample survival analysis among different immune subtypes, including OS and PFS. C. Heat map showing activity levels of oncogenic features among immune subtypes. The activity levels of oncogenic characteristics were calculated using the ssGSEA method.

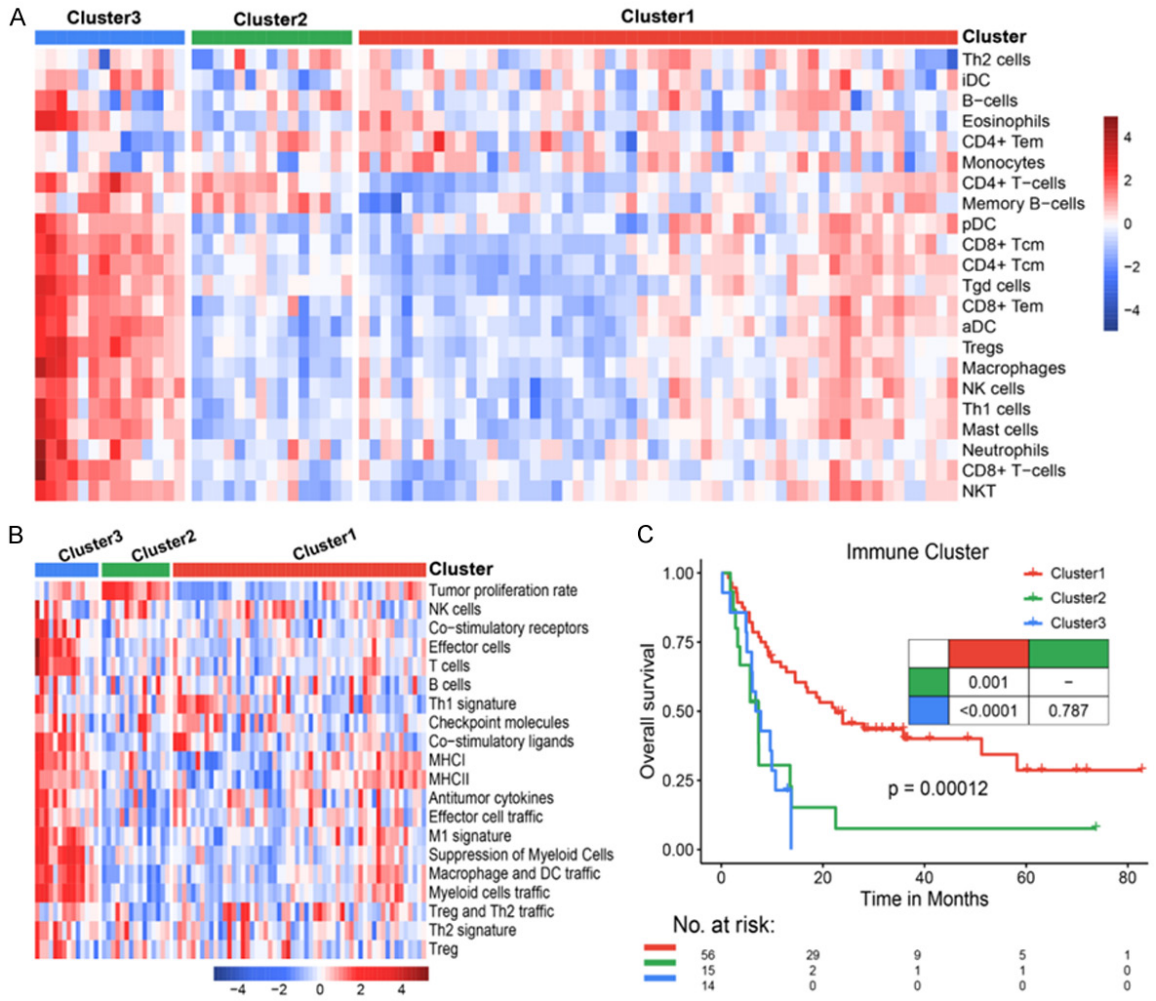

Figure 2. Unsupervised hierarchical cluster analysis based on immune activity levels in validation set and the clinical relevance analysis. A. Unsupervised hierarchical cluster analysis based on immune activity level in validation set (GSE4412-GBM sample). The level of immune activity was calculated using the ssGSEA method. B. Heat map display of immune signature activity levels. The level of immune activity was calculated using the ssGSEA method. C. Kaplan-Meier curve represents survival analysis between subtypes of confirmatory concentrated immunity.

These results indicated that GBM can be classified into subtypes based on the level of immune cell infiltration.

Validation analysis of the immune subtypes in GBM

To confirm the conservation of these immune subtypes in GBM, we downloaded a data set of 85 GBM samples as an independent validation set. The infiltration level of the gene set of 22 immune cell markers, according to previous studies, was calculated using ssGSEA. Using unsupervised hierarchical cluster analysis, the GBM samples were grouped into three Clusters: Cluster 1 with 55 samples, Cluster 2 with 15 samples, and Cluster 3 with 14 samples. Among these Clusters, patients in Cluster 3 showed the highest immunoactivity (**Figure 2A**). We obtained immune signatures of TMEs from previous studies and found that the activity level of immune signatures was the highest in Cluster 3, which was consistent with hierarchical clustering (**Figure 2B**). In addition, based on this validation set data, we also found that patients' OS showed significant differences among different immune subtypes, and OS was significantly worse in Clusters 3 than Cluster 1 (**Figure 2C**).

These results indicate that the immune subtypes in GBM is conserved.

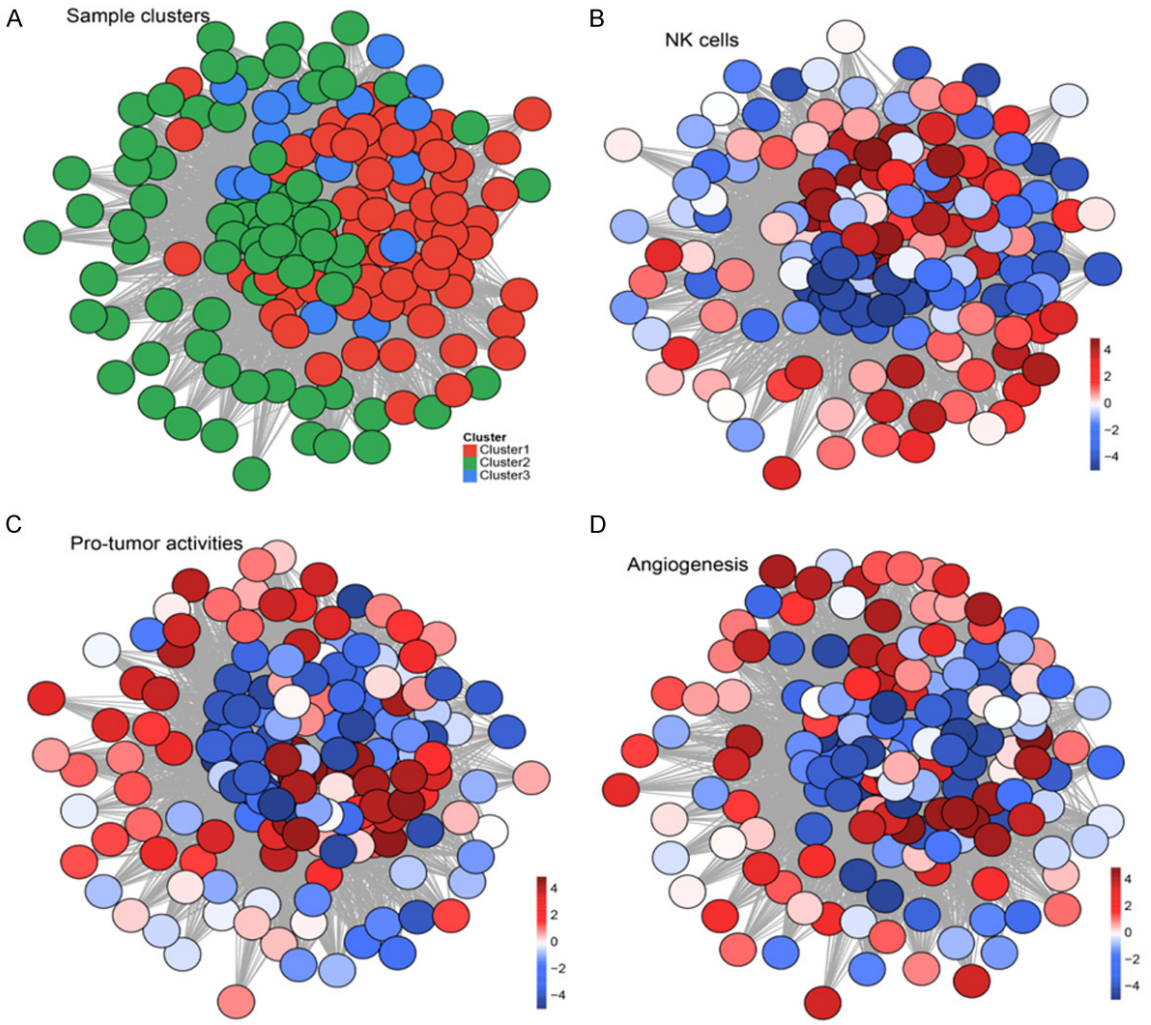

Figure 3. Louvain community classification analysis. A. Louvain community classification map shows the classification of different immune subtypes of GBM samples. B-D. Natural killer cell activity, oncogenic characteristic activity, and angiogenic activity level in DIFFERENT immune subtypes of GBM samples. The activity levels of each feature was calculated using the ssGSEA method. The bluer the color, the lower the activity, and the redder the color, the higher the activity.

Characteristics of TME among immune subtypes

To explore the characteristics of the TME among these immune subtypes, we first used the Louvain community classification method to conduct a classification analysis of GBM samples, and these GBM samples were mapped as immune subtypes into the Louvain community classification (**Figure 3A**). Next, we described the distribution of the activity levels of some immune and oncogenic traits in different immune subtypes. The results showed that the natural killer cells (**Figure 3B**), oncogenic features (**Figure 3C**), and angiogenic features (**Figure 3D**) showed higher activity levels in Cluster 3 patients. Next, we demonstrated the distribution of immunoactivity and the activity levels of oncogenic characteristics among different immune subtypes using a box diagram. The results showed that there were significant differences in immunoactivity and activity levels of oncogenic traits, and the patients in Cluster 3 had significantly stronger immune score, matrix score, CYT activity and IFN-γ activity, as well as the tumor-associated fibroblasts activity and angiogenesis activity (**Figure 4A-F**). However, the patients in Cluster 1 showed significantly lower levels of the above immunoactivity and oncogenic characteristics.

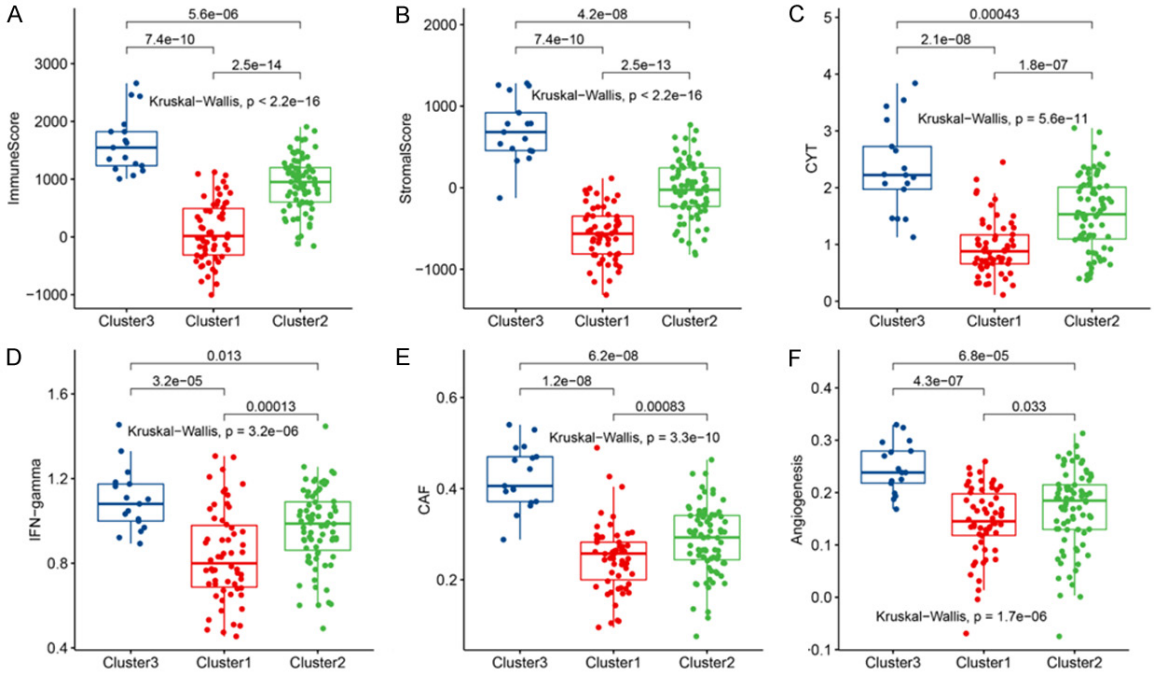

Figure 4. Box diagram distribution of TME and oncogenic characteristics among different immune subtypes in GBM samples. A-F. immune score, stromal score, CYT activity and IFN-γ activity, cancer-associated fibroblasts (CAF) activity and angiogenesis activity. Kruskal-Wallias test was used for significance analysis between multiple groups, and Wilcoxon rank sum test was used for significance analysis between two groups.

Thus, these results indicate that the activation of immune infiltration in GBM is accompanied by active pro-cancer features.

Clinical features and independent prognostic efficacy among immune subtypes

We described the distribution of clinical features among the different immune subtypes, including age, sex, and whether radiotherapy had been administered. We also described the correlation between immune subtypes and GBM sample expression subtypes, MGMT methylation status, and IDH1/TP53/EGFR mutation status (**Figure 5A**). The results showed that patients in Clusters 1 and 3 were more likely to be male, accounting for 61.4% and 85.7% of patients, respectively, whereas the proportion of male patients in Cluster2 subtype was 53.7%. The age distribution results showed patients in Cluster 2 were more likely to be elderly patients (age > 60 years), accounting for 61.1%, whereas Clusters 1 and 3 patients accounted for 43.2% and 57.1%, respectively. Genome mutation analysis revealed that patients in Cluster 1 were more likely to carry EGFR mutations (39.7%), whereas patients in Cluster 3 were more likely to carry TP53 mutations (41.2%). Through MGMT methylation status analysis, we found that patients in Cluster 1 were more prone to MGMT methylation, accounting for 12.3%, whereas patients in Clusters 2 and 3 accounted for 3.9% and 0%, respectively. Analysis of known expression spectrum subtypes showed that patients in Cluster 1 were more likely to belong to the classical and proneural subtypes, accounting for 49.1% and 31.6%, respectively. Patients in Cluster 3 were more likely to belong to the mesenchymal subtype, accounting for 93.8%. Notably, a significant correlation was observed between the immune subtypes and subtypes with known expression profiles.

We then analyzed the prognostic efficacy of the immune subtypes and found that Cluster 3 was a significant risk factor, with worse OS (**Figure 5B**) and PFS (**Figure 5C**) than Cluster 1. Moreover, Cluster 2 was a significant risk factor for worse PFS than Cluster 1 (**Figure 5C**). Next, we adjusted for the effects of clinical factors (including age, sex, and radiotherapy) and found that Cluster 3 had a worse OS (**Figure 5D**) and PFS (**Figure 5E**) than Cluster 1 as an independent risk factor.

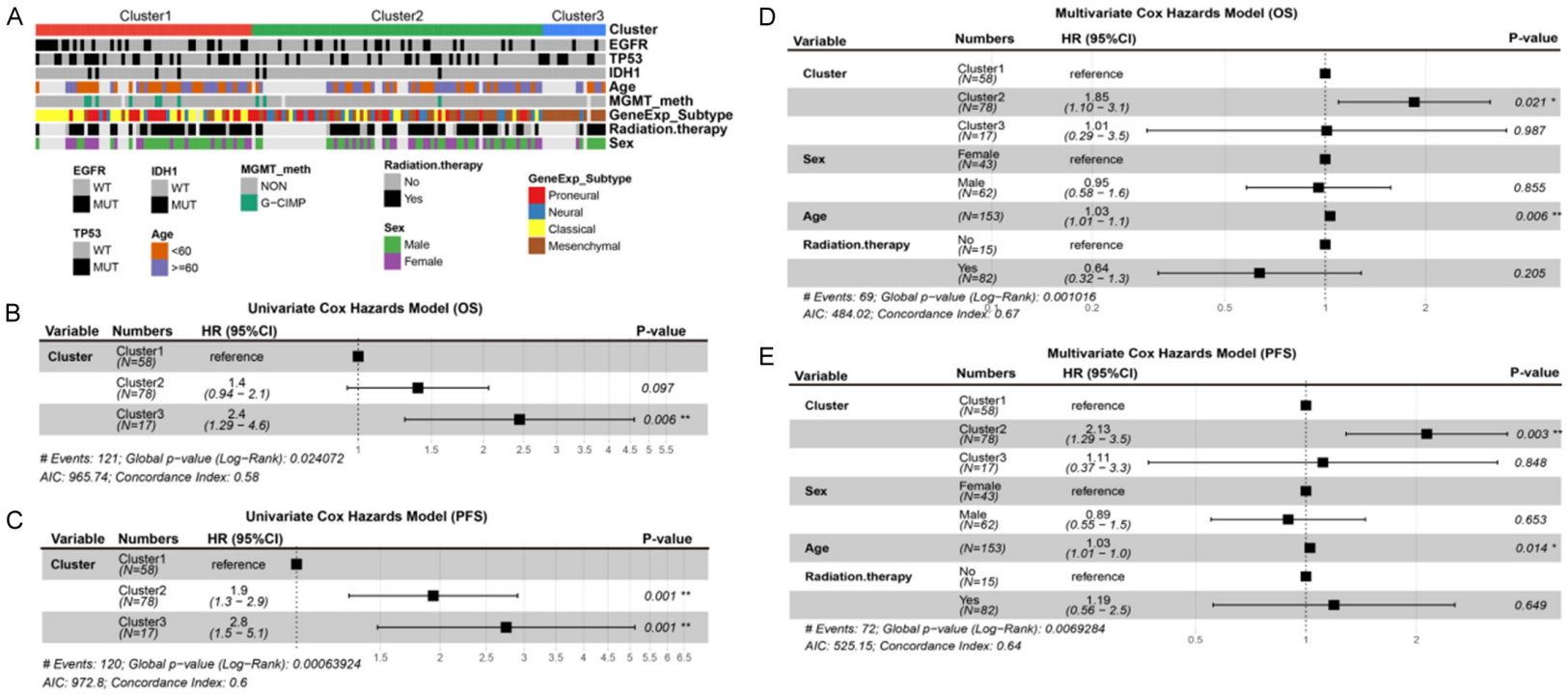

Figure 5. Distribution of clinical feature and Cox regression analysis for survival. A. Distribution of clinical features among different immune subtypes. B, C. Univariate Cox regression analysis among different immune subtypes, including OS and PFS. D, E. Multivariate Cox regression analysis between different immune subtypes, including OS and PFS after adjusting for clinical factors.

These results suggest that GBM immune subtypes have independent prognostic efficacy.

Enrichment analysis of functional pathways of differential genes between immune subtypes

To explore the underlying mechanism for driving these three immune-specific types in GBM, we performed the enrichment analysis of differentially expressed genes according to the expression level of genes in immune subtypes, and differentially expressed genes among subtypes were screened according to thresholds (FC ≥ 1.5 or FC ≤ 2/3, FDR ≤ 0.05). We obtained 137 differentially expressed genes of the GBM immune subtypes by the intersection of differentially expressed genes of the three subtypes. Functional enrichment analysis was conducted on genes differentially expressed in the GBM immune subtypes, which were enriched in 61 BP, 21 MF, 11 CC, and 24 KEGG pathways. The top 15 GO terms and Top 20 Pathways were screened and displayed according to their significance rankings. GO terms showed that GBM immune subtype-specific differentially expressed genes were mainly enriched in extracellular matrix organization and signaling receptor regulator activity (**Figure 6A-C**). KEGG pathway terms showed that PI3K-Akt signaling Pathway and TGF-β signaling pathways were mainly enriched (**Figure 6D**).

Thus, these results indicated that there were significant differences in the expression patterns of genes involved in driving these specific immune infiltration subtypes.

Immune subtype-specific TFs regulatory network contributes to drug sensitivity analysis

Because of the significant differences in the expression patterns of the genes involved in driving these specific immune infiltration subtypes, we further explored the related TFs. Based on the Viper algorithm, we identified the master regulator and specific TF of each immune subtype. The result showed that Clusters 1, 2, and 3 contained 29, 18, and 64 specific TFs, respectively. Next, we calculated the mutual information between these TFs based on their expression levels and constructed a regulatory network among these TFs (**Figure 7**). For example, The TF. SMARCA of Cluster 1 has a mutual regulatory relationship with multiple the TF. TFZNF696 in Cluster 2 and TF. TCF7L2 of Cluster 1 internal subtype, EWSR1 and other subtypes, and TF. PKNOX2 and TF. SREBF2 in Cluster 3 (**Figure 7**). In addition, **Figure 7** shows that subtype-specific TFs are more prone to internal TFs regulation.

To explore the drug sensitivity based on the above TFs, pharmacogenomic data were downloaded from the GDSC, and ridge regression was used to predict drug sensitivity in patients with GBM based on lung adenocarcinoma cell line expression data and drug response information (logIC50). By analyzing the correlation between the expression levels of each immune subgroup-specific TFs and drug sensitivity, we found that different immune subtype-specific TFs presented different correlation patterns with the drugs (**Figure 8**). For Cluster 2-specific TFs, the expression level showed a significant negative correlation with drugs, such as TGIF2 and temozolomide, commonly used as anticancer drugs for GBM. Cluster 1-specific TFs showed significant correlation with more drugs, especially positive correlation with some drugs, such as the PI3K/MTOR drugs temsirolimus and GSK690693 and IGF1R inhibitor BMS-536924. However, there was no significant correlation between Cluster 3-specific TFs and their susceptibility to these drugs, indicating that GBM in Cluster 3 is refractory. Only four drugs-obatoclax mesylate, NPK76-II-72-1, gemcitabine, and TAK-715-were significantly correlated with Cluster 3-specific TFs.

Thus, these results indicate that TFs that drive the formation of different subtypes of immune infiltration are specific, and that differences in TFs affect therapeutic sensitivity to drugs. GBM cells which with high immune-infiltration activity have poor drug sensitivity.

Discussion

GBM is the most aggressive malignant tumor of human central nervous system; however, its prognosis is poor [7]. It should be noted that there is a significant difference in the survival prognosis of patients with GBM. One important reason is that patients with GBM have large differences in sensitivity to postoperative adjuvant drug therapy. The classification of immune subtypes and clinical significance of gliomas have been extensively studied in recent years. Zhou's study revealed that diffuse gliomas could be divided into different immune-associ-

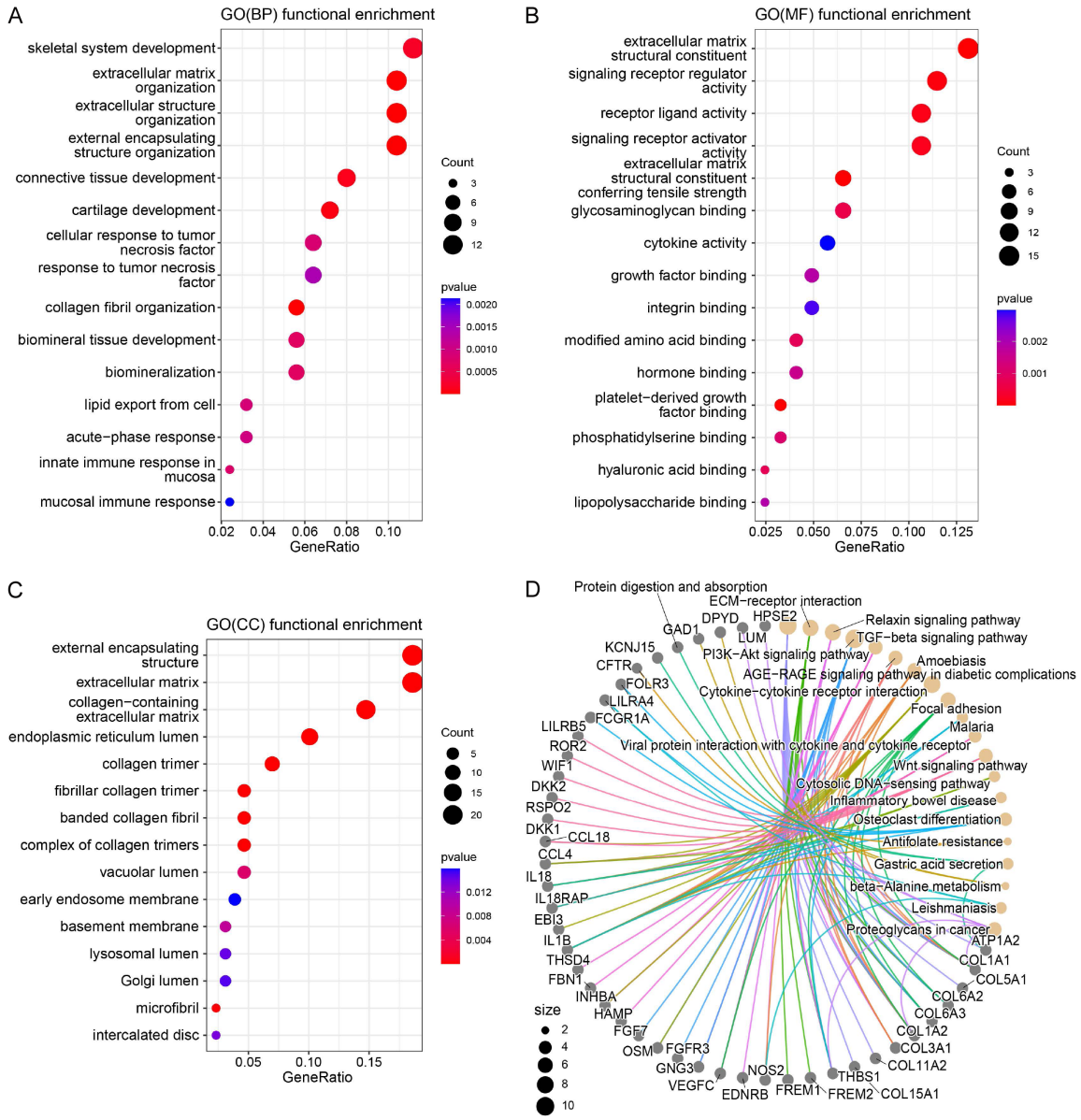

Figure 6. Enrichment analysis of various differentially expressed genes among GBM immune subtypes. A-C. BP, MF and CC of differentially expressed genes among GBM immune subtypes obtained by GO enrichment analysis. Top15 GO terms were extracted according to the significance level for display. D. KEGG enrichment was performed for differentially expressed genes between immune subtypes, and the top 20 pathways were extracted and displayed according to the significance level. The dot in the figure represents a gene or pathway, the line indicates that the gene is in a pathway, and the size of the pathway points indicates the number of genes in the pathway.

ated subtypes based on the expression profiling of immune-related genes, and they demonstrated that these immune-associated subtypes could independently predict the clinical prognosis and provide potential immunotherapy targets for diffuse gliomas [24]. Zhu's study found that lower-grade gliomas could be divided into four immunotypes, and the "immune-rich" subtype that exhibits the highest immune infiltration indicates poor survival expectation [25]. However, few reports exist on the classification of the immune-infiltrating subtypes of GBM and their sensitivity to drug therapy.

In this study, we found that GBMs can be conservatively divided into three immune subtypes based on the level of immune cell infiltration inside the tumor: immunosuppressed, moderate immunoactivity, and high immunoactivity. Clinical relevance shown that a high level of

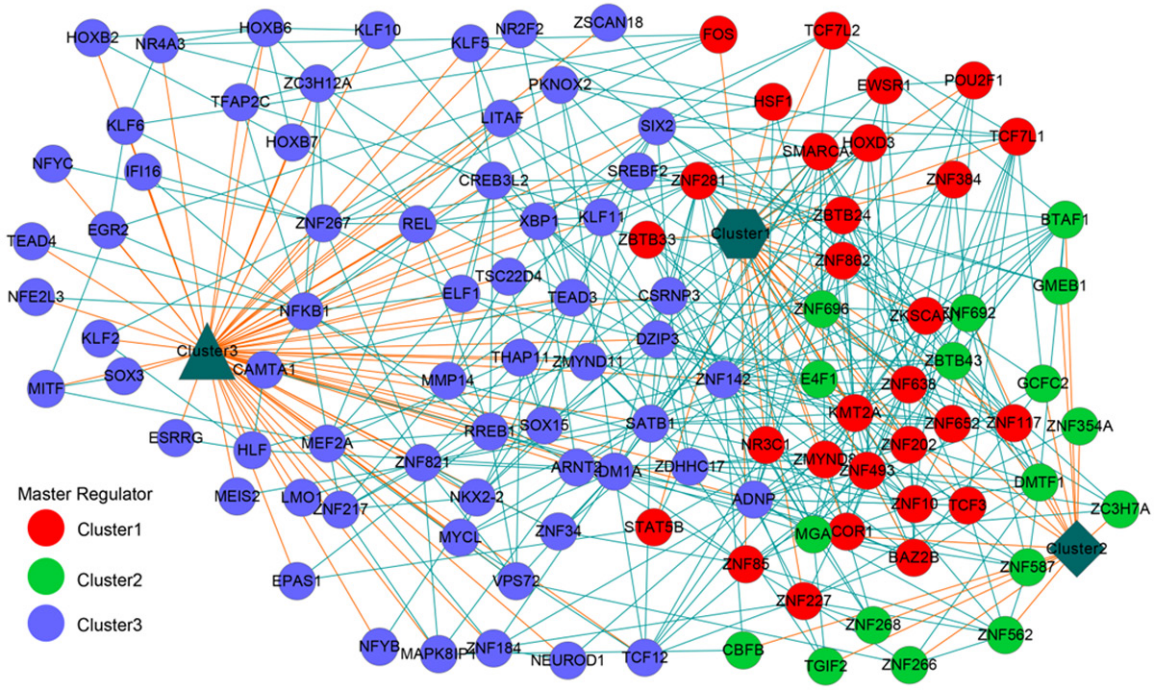

Figure 7. Regulatory relationships among TFs specific to immune subtypes. Red: Cluster 1 specific TF; Green: Cluster 2 specific TF; Blue: Cluster 3 specific TF. The orange line represents the immune subtype TF belongs to; the grass green line represents the regulatory relationship between TF based on mutual information analysis.

immune cells infiltrating is associated with poor survival outcomes, including OS and PFS. Previous studies have shown that immune infiltration in the TME affects cancer progression and patient prognosis, and that tumor-infiltrating immune cells could be an independent predictor of cancer prognosis [26, 27]. In most cases, tumors with high immune activity are associated with better prognosis [28]; however, our study indicated a contrasting phenomenon. Similar studies have reported that high immune activity or immune cell infiltration is associated with worse prognosis in certain cancer types, including gliomas [29-31]. Matsuo found that higher immune activity was associated with worse OS in patients with uveal melanoma and low-grade glioma, and the underlying mechanism is that epithelial or endothelial mesenchymal transition was mainly induced in retinal pigment cells or endothelial cells that comprise the blood-retinal and blood-brain barriers, which are unique structures of the eye and central nervous system, respectively. Furthermore, the expression of inflammatory chemokines, particularly CCL5, was strongly correlated with immune activity and was associated with poor survival, particularly in these cancers [32]. Our study revealed that GBM with high immune activity exhibited much stronger oncogenic characteristics, including angiogenesis, endothelium, matrix remodeling, cancer-associated fibroblasts, matrix, neutrophil signature, tumor-associated macrophages, protumor cytokines, and granulocyte traffic.

Owing to the above relationship, immune-associated subtypes have independent prognostic efficacy in GBM. Based on these results, we were interested in the molecular signaling pathways are involved in driving the emergence of immune-associated subtypes in GBM and how these molecular signaling pathways affect the therapeutic outcome of GBM. We performed enrichment analysis of differentially expressed genes according to their expression levels in these immune-specific subtypes. We found that GBM immune subtype specific differentially expressed genes were mainly enriched through biological processes and pathways which are highly correlated with cancer immune microenvironment and clinical prognosis, including extracellular matrix organization and signaling receptor regulator activity, PI3K-Akt signaling pathway, ECM-receptor interaction,

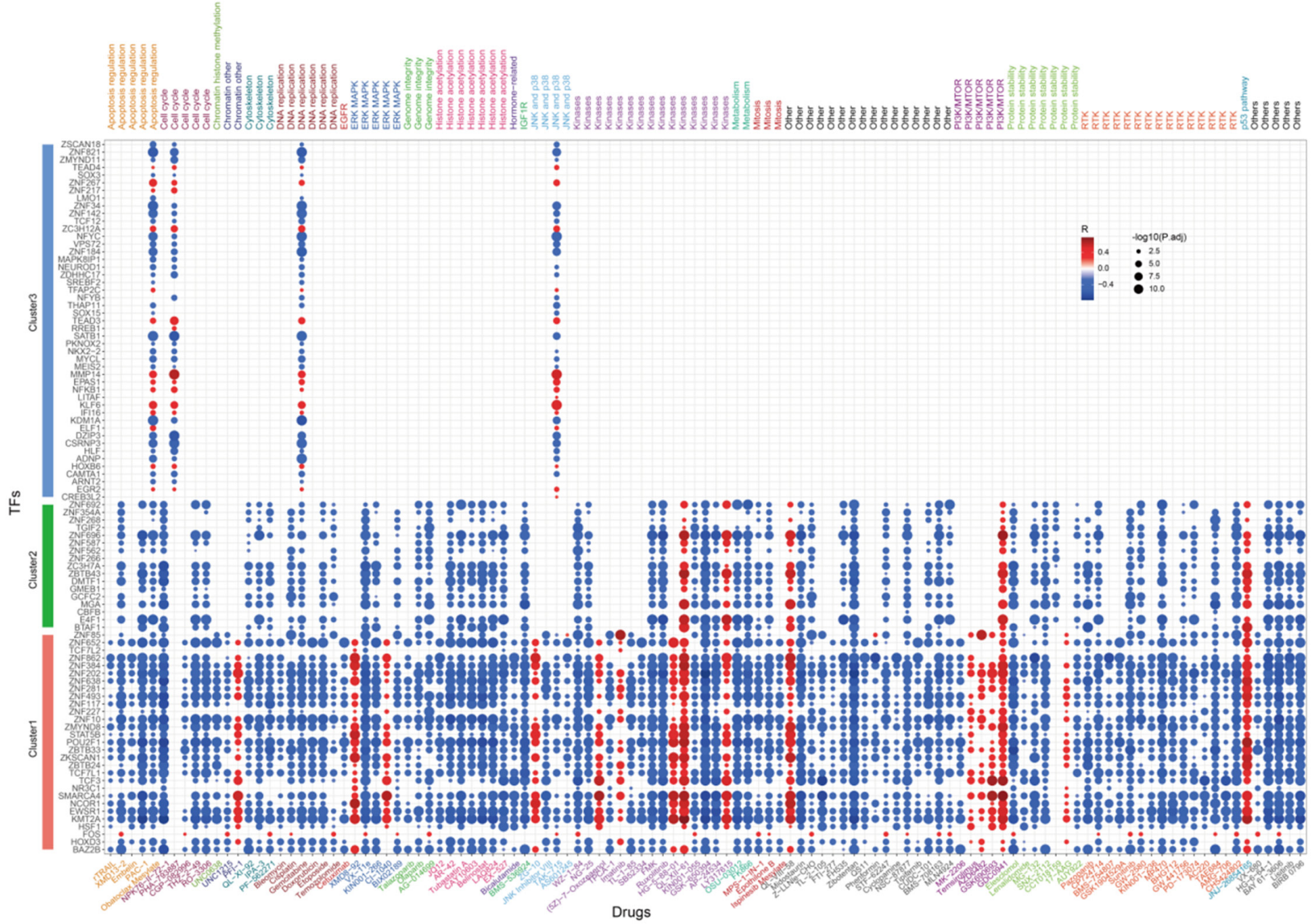

Figure 8. Correlation analysis between immune subtype-specific TF and drug sensitivity. Different TF colors indicate different immune subtypes, and different drugs indicate different drug target gene pathways.

Wnt signaling pathway, and TGF-β signaling pathway. The PI3K-Akt signaling pathway that regulates the immune and inflammatory responses in glioma and other cancers has been identified, and this pathway regulates the sensitivity to immunotherapy [33-36]. The ECM-receptor interaction pathway was found to be highly correlated with immune cell-related pathways in ovarian cancer and had significant prognostic differences and immunological characteristics [37]. The Wnt signaling pathway is involved in regulating the treatment outcome of IDH1 wild-type glioblastoma, as blocking the Wnt signaling pathway could improving the hostile immunosuppressive microenvironment [38]. The TGF-β signaling pathway is also involved in glioma immune microenvironment by regulating the regulatory T cells and further promoting glioma cell stemness [39]. The TGF-β signaling pathway have been shown to mediate immune suppression, and its inhibition could restore the immune surveillance in glioma models [40]. These results revealed the critical signaling pathways that drive the construction of immune subtypes in GBM.

To explain how these immune-associated signaling pathways affect the sensitivity of GBM to chemotherapy, we analyzed the characteristics of TFs upstream of the signaling pathway and identified TFs specific to different immune subtypes. The result revealed that specific TFs are important factors driving the formation of different immune subtypes in GBM, and that these TFs are prone to internal regulation. Among these immune subtype-specific TFs, 29 TFs driving the construction of a high immunoactivity microenvironment showed no obvious drug sensitivity to most anticancer compounds, and did not react with these TFs. However, TFs that drive the immunosuppressive and moderate immunoactivity immune subtypes showed significant sensitivity to anticancer compounds, including temozolomide. Since MGMT methylation status is an important indicator for predicting the sensitivity of temozolomide chemotherapy in patients with GBM, we also evaluated the correlation between the driving TFs of different immune statuses and the methylation status of MGMT, and found that the TFs driving the construction of a high immunoactivity microenvironment in cluster 3 were prone to the unmethylated status of MGMT compared to the other two clusters.

In this study, we also found four drugs with potential therapeutic value for GBM that exhibited a high immunoactivity microenvironment: obatoclax mesylate, NPK76-II-72-1, gemcitabine, TAK-715. Obatoclax mesylate is a Bcl-2 family antagonist that exhibits anti-tumor effects in small-cell and non-small cell lung cancers [41-43]. Previous studies have indicated that Bcl-2 inhibitors, including obatoclax mesylate, can restore temozolomide sensitivity and inhibit GBM stem-like cells [44, 45]. NPK76-II-72-1 regulates the cell cycle by targeting PLK3, which has a lower IC50 in GBM than in glioma according to the GDSC dataset. However, there are few reports on its therapeutic effects in GBM. Gemcitabine is an inhibitor of DNA replication that mostly exhibits clinical value in pancreatic cancer, non-small cell lung cancers, breast cancer, and ovarian cancer [46-49]. Gemcitabine has also been reported to have an adjuvant therapeutic effect on gliomas [50, 51]. TAK-715 is an inhibitor of p38 MAP kinase [52], and p38 MAP kinase plays an important role in cancer, such as stemness maintenance of cancer cells and cancer metastasis, indicating that TAK-71 has a potential anti-tumor effect; however, there are few reports to date [53]. Thus, these results suggest a potential therapeutic drug for the refractory GBM.

In summary, this is the first study to explore the relationship between the clinical prognosis of GBM and the level of immune infiltration. The activation of immune infiltration is closely related to the poor prognosis of GBM, and the level of immune infiltration can be used as an independent predictor of the clinical prognosis of GBM. Secondly, we analyzed the correlation between drug sensitivity and TFs and found that the relevant TFs that drive the activation of immune infiltration subtypes were significantly correlated with the insensitivity of GBM to chemical drugs. Most importantly, we identified four drugs for refractory GBM treatment, which may provide new clues for the personalized treatment of GBM in the future.

Acknowledgements

This work was supported by a grant from Three design projects in Shenzhen (SZSM20162008) and Shenzhen Science and Technology Innovation Committee Projects (No. JCYJ202205-31094202006).

Disclosure of conflict of interest

None.

Address correspondence to: Baodong Chen, Department of Neurosurgery, Peking University Shenzhen Hospital, Shenzhen Peking University-The Hong Kong University of Science and Technology Medical Center, 1120 Lianhua Road, Futian District, Shenzhen 518036, Guangdong, P. R. China. Tel: +86-13602593425; Fax: +86-0755-8392; E-mail: puszh_chenbd@163.com; Ruxiang Xu, Department of Neurosurgery, Sichuan Academy of Medical Science and Sichuan Provincial People's Hospital, University of Electronic Science and Technology of China, 32 West Second Section, First Ring Road, Qingyang District, Chengdu 610072, Sichuan, P. R. China. Tel: +86-13391788118; Fax: +86-0288-7394; E-mail: smuxuruxiang@163.com

References

[1] Tan AC, Ashley DM, Lopez GY, Malinzak M, Friedman HS and Khasraw M. Management of glioblastoma: state of the art and future directions. CA Cancer J Clin 2020; 70: 299-312.

[2] Ostrom QT, Cioffi G, Waite K, Kruchko C and Barnholtz-Sloan JS. CBTRUS statistical report: primary brain and other central nervous system tumors diagnosed in the United States in 2014-2018. Neuro Oncol 2021; 23 Suppl 2: iii1-iii105.

[3] Chen J, Li Y, Yu TS, McKay RM, Burns DK, Kernie SG and Parada LF. A restricted cell population propagates glioblastoma growth after chemotherapy. Nature 2012; 488: 522-526.

[4] van Solinge TS, Nieland L, Chiocca EA and Broekman MLD. Advances in local therapy for glioblastoma - taking the fight to the tumour. Nat Rev Neurol 2022; 18: 221-236.

[5] Sanmamed MF and Chen L. A paradigm shift in cancer Immunotherapy: from enhancement to normalization. Cell 2019; 176: 677.

[6] Carlsson SK, Brothers SP and Wahlestedt C. Emerging treatment strategies for glioblastoma multiforme. EMBO Mol Med 2014; 6: 1359-1370.

[7] von Neubeck C, Seidlitz A, Kitzler HH, Beuthien-Baumann B and Krause M. Glioblastoma multiforme: emerging treatments and stratification markers beyond new drugs. Br J Radiol 2015; 88: 20150354.

[8] Filley AC, Henriquez M and Dey M. Recurrent glioma clinical trial, CheckMate-143: the game is not over yet. Oncotarget 2017; 8: 91779-91794.

[9] Omuro A, Vlahovic G, Lim M, Sahebjam S, Baehring J, Cloughesy T, Voloschin A, Ramkissoon SH, Ligon KL, Latek R, Zwirtes R, Strauss L, Paliwal P, Harbison CT, Reardon DA and Sampson JH. Nivolumab with or without ipilimumab in patients with recurrent glioblastoma: results from exploratory phase I cohorts of CheckMate 143. Neuro Oncol 2018; 20: 674-686.

[10] Reiss SN, Yerram P, Modelevsky L and Grommes C. Retrospective review of safety and efficacy of programmed cell death-1 inhibitors in refractory high grade gliomas. J Immunother Cancer 2017; 5: 99.

[11] Kurz SC, Cabrera LP, Hastie D, Huang R, Unadkat P, Rinne M, Nayak L, Lee EQ, Reardon DA and Wen PY. PD-1 inhibition has only limited clinical benefit in patients with recurrent high-grade glioma. Neurology 2018; 91: e1355-e1359.

[12] Hoadley KA, Yau C, Hinoue T, Wolf DM, Lazar AJ, Drill E, Shen R, Taylor AM, Cherniack AD, Thorsson V, Akbani R, Bowlby R, Wong CK, Wiznerowicz M, Sanchez-Vega F, Robertson AG, Schneider BG, Lawrence MS, Noushmehr H, Malta TM; Cancer Genome Atlas Network; Stuart JM, Benz CC and Laird PW. Cell-of-origin patterns dominate the molecular classification of 10,000 tumors from 33 types of cancer. Cell 2018; 173: 291-304, e296.

[13] Martin ML, Zeng Z, Adileh M, Jacobo A, Li C, Vakiani E, Hua G, Zhang L, Haimovitz-Friedman A, Fuks Z, Kolesnick R and Paty PB. Logarithmic expansion of LGR5(+) cells in human colorectal cancer. Cell Signal 2018; 42: 97-105.

[14] Bindea G, Mlecnik B, Tosolini M, Kirilovsky A, Waldner M, Obenauf AC, Angell H, Fredriksen T, Lafontaine L, Berger A, Bruneval P, Fridman WH, Becker C, Pages F, Speicher MR, Trajanoski Z and Galon J. Spatiotemporal dynamics of intratumoral immune cells reveal the immune landscape in human cancer. Immunity 2013; 39: 782-795.

[15] Aran D, Hu Z and Butte AJ. xCell: digitally portraying the tissue cellular heterogeneity landscape. Genome Biol 2017; 18: 220.

[16] Bagaev A, Kotlov N, Nomie K, Svekolkin V, Gafurov A, Isaeva O, Osokin N, Kozlov I, Frenkel F, Gancharova O, Almog N, Tsiper M, Ataullakhanov R and Fowler N. Conserved pan-cancer microenvironment subtypes predict response to immunotherapy. Cancer Cell 2021; 39: 845-865, e847.

[17] Becht E, Giraldo NA, Lacroix L, Buttard B, Elarouci N, Petitprez F, Selves J, Laurent-Puig P, Sautes-Fridman C, Fridman WH and de Reynies A. Estimating the population abundance of tissue-infiltrating immune and stromal cell populations using gene expression. Genome Biol 2016; 17: 218.

[18] Li T, Fu J, Zeng Z, Cohen D, Li J, Chen Q, Li B and Liu XS. TIMER2.0 for analysis of tumor-infiltrating immune cells. Nucleic Acids Res 2020; 48: W509-W514.
[19] Yoshihara K, Shahmoradgoli M, Martinez E, Vegesna R, Kim H, Torres-Garcia W, Trevino V, Shen H, Laird PW, Levine DA, Carter SL, Getz G, Stemke-Hale K, Mills GB and Verhaak RG. Inferring tumour purity and stromal and immune cell admixture from expression data. Nat Commun 2013; 4: 2612.
[20] Gao Z, Tao Y, Lai Y, Wang Q, Li Z, Peng S, Chen J, Cai W, Li K and Huang H. Immune cytolytic activity as an indicator of immune checkpoint inhibitors treatment for prostate cancer. Front Bioeng Biotechnol 2020; 8: 930.
[21] Takahashi H, Kawaguchi T, Yan L, Peng X, Qi Q, Morris LGT, Chan TA, Tsung A, Otsuji E and Takabe K. Immune cytolytic activity for comprehensive understanding of immune landscape in hepatocellular carcinoma. Cancers (Basel) 2020; 12: 1221.
[22] Alvarez MJ, Shen Y, Giorgi FM, Lachmann A, Ding BB, Ye BH and Califano A. Functional characterization of somatic mutations in cancer using network-based inference of protein activity. Nat Genet 2016; 48: 838-847.
[23] Geeleher P, Cox NJ and Huang RS. Clinical drug response can be predicted using baseline gene expression levels and in vitro drug sensitivity in cell lines. Genome Biol 2014; 15: R47.
[24] Zhou Q, Yan X, Liu W, Yin W, Xu H, Cheng D, Jiang X and Ren C. Three immune-associated subtypes of diffuse glioma differ in immune infiltration, immune checkpoint molecules, and prognosis. Front Oncol 2020; 10: 586019.
[25] Zhu Y, Feng S, Song Z, Wang Z and Chen G. Identification of immunological characteristics and immune subtypes based on single-sample gene set enrichment analysis algorithm in lower-grade glioma. Front Genet 2022; 13: 894865.
[26] Galon J, Costes A, Sanchez-Cabo F, Kirilovsky A, Mlecnik B, Lagorce-Pages C, Tosolini M, Camus M, Berger A, Wind P, Zinzindohoue F, Bruneval P, Cugnenc PH, Trajanoski Z, Fridman WH and Pages F. Type, density, and location of immune cells within human colorectal tumors predict clinical outcome. Science 2006; 313: 1960-1964.
[27] Jiang S, Ding X, Wu Q, Cheng T, Xu M and Huang J. Identifying immune cells-related phenotype to predict immunotherapy and clinical outcome in gastric cancer. Front Immunol 2022; 13: 980986.
[28] Haanen J. Converting cold into hot tumors by combining immunotherapies. Cell 2017; 170: 1055-1056.
[29] Lu J, Peng Y, Huang R, Feng Z, Fan Y, Wang H, Zeng Z, Ji Y, Wang Y and Wang Z. Elevated TYROBP expression predicts poor prognosis and high tumor immune infiltration in patients with low-grade glioma. BMC Cancer 2021; 21: 723.
[30] Shi H, Song Y, Song Z and Huang C. CKMT1B is a potential prognostic biomarker and associated with immune infiltration in Lower-grade glioma. PLoS One 2021; 16: e0245524.
[31] Hao YP, Wang WY, Qiao Q and Li G. EFNA1 is a potential key gene that correlates with immune infiltration in low-grade glioma. Medicine (Baltimore) 2021; 100: e26188.
[32] Matsuo H, Kamatani T, Hamba Y, Boroevich KA and Tsunoda T. Association between high immune activity and worse prognosis in uveal melanoma and low-grade glioma in TCGA transcriptomic data. BMC Genomics 2022; 23: 351.
[33] Han S, Wang PF, Cai HQ, Wan JH, Li SW, Lin ZH, Yu CJ and Yan CX. Alterations in the RTK/Ras/PI3K/AKT pathway serve as potential biomarkers for immunotherapy outcome of diffuse gliomas. Aging (Albany NY) 2021; 13: 15444-15458.
[34] Cao X, Zhou Y, Mao F, Lin Y, Zhou X and Sun Q. Identification and characterization of three Siglec15-related immune and prognostic subtypes of breast-invasive cancer. Int Immunopharmacol 2022; 106: 108561.
[35] Wang Z, Wang X, Xu Y, Li J, Zhang X, Peng Z, Hu Y, Zhao X, Dong K, Zhang B, Gao C, Zhao X, Chen H, Cai J, Bai Y, Sun Y and Shen L. Mutations of PI3K-AKT-mTOR pathway as predictors for immune cell infiltration and immunotherapy efficacy in dMMR/MSI-H gastric adenocarcinoma. BMC Med 2022; 20: 133.
[36] Mafi S, Mansoori B, Taeb S, Sadeghi H, Abbasi R, Cho WC and Rostamzadeh D. mTOR-mediated regulation of immune responses in cancer and tumor microenvironment. Front Immunol 2021; 12: 774103.
[37] Liu X, Gao J, Wang J, Chu J, You J and Jin Z. Identification of two molecular subtypes of dysregulated immune lncRNAs in ovarian cancer. Exp Biol Med (Maywood) 2021; 246: 547-559.
[38] Fan D, Yue Q, Chen J, Wang C, Yu R, Jin Z, Yin S, Wang Q, Chen L, Liao X, Peng C, Zhang J, Cao Z, Mao Y, Huang R, Chen L and Li C. Reprogramming the immunosuppressive microenvironment of IDH1 wild-type glioblastoma by blocking Wnt signaling between microglia and cancer cells. Oncoimmunology 2021; 10: 1932061.
[39] Liu S, Zhang C, Wang B, Zhang H, Qin G, Li C, Cao L, Gao Q, Ping Y, Zhang K, Lian J, Zhao Q, Wang D, Zhang Z, Zhao X, Yang L, Huang L, Yang B and Zhang Y. Regulatory T cells pro-

mote glioma cell stemness through TGF-beta-NF-kappaB-IL6-STAT3 signaling. Cancer Immunol Immunother 2021; 70: 2601-2616.
[40] Tran TT, Uhl M, Ma JY, Janssen L, Sriram V, Aulwurm S, Kerr I, Lam A, Webb HK, Kapoun AM, Kizer DE, McEnroe G, Hart B, Axon J, Murphy A, Chakravarty S, Dugar S, Protter AA, Higgins LS, Wick W, Weller M and Wong DH. Inhibiting TGF-beta signaling restores immune surveillance in the SMA-560 glioma model. Neuro Oncol 2007; 9: 259-270.
[41] Chiappori A, Williams C, Northfelt DW, Adams JW, Malik S, Edelman MJ, Rosen P, Van Echo DA, Berger MS and Haura EB. Obatoclax mesylate, a pan-bcl-2 inhibitor, in combination with docetaxel in a phase 1/2 trial in relapsed non-small-cell lung cancer. J Thorac Oncol 2014; 9: 121-125.
[42] Paik PK, Rudin CM, Pietanza MC, Brown A, Rizvi NA, Takebe N, Travis W, James L, Ginsberg MS, Juergens R, Markus S, Tyson L, Subzwari S, Kris MG and Krug LM. A phase II study of obatoclax mesylate, a Bcl-2 antagonist, plus topotecan in relapsed small cell lung cancer. Lung Cancer 2011; 74: 481-485.
[43] Schimmer AD, O'Brien S, Kantarjian H, Brandwein J, Cheson BD, Minden MD, Yee K, Ravandi F, Giles F, Schuh A, Gupta V, Andreeff M, Koller C, Chang H, Kamel-Reid S, Berger M, Viallet J and Borthakur G. A phase I study of the pan bcl-2 family inhibitor obatoclax mesylate in patients with advanced hematologic malignancies. Clin Cancer Res 2008; 14: 8295-8301.
[44] Berghauser Pont LM, Spoor JK, Venkatesan S, Swagemakers S, Kloezeman JJ, Dirven CM, van der Spek PJ, Lamfers ML and Leenstra S. The Bcl-2 inhibitor obatoclax overcomes resistance to histone deacetylase inhibitors SAHA and LBH589 as radiosensitizers in patient-derived glioblastoma stem-like cells. Genes Cancer 2014; 5: 445-459.
[45] Yu J, Han L, Yang F, Zhao M, Zhou H and Hu L. SOCS5 contributes to temozolomide resistance in glioblastoma by regulating Bcl-2-mediated autophagy. Bioengineered 2022; 13: 14125-14137.
[46] Stovgaard ES, Asleh K, Riaz N, Leung S, Gao D, Nielsen LB, Laenkholm AV, Balslev E, Jensen MB, Nielsen D and Nielsen TO. The immune microenvironment and relation to outcome in patients with advanced breast cancer treated with docetaxel with or without gemcitabine. Oncoimmunology 2021; 10: 1924492.
[47] Konstantinopoulos PA, Cheng SC, Wahner Hendrickson AE, Penson RT, Schumer ST, Doyle LA, Lee EK, Kohn EC, Duska LR, Crispens MA, Olawaiye AB, Winer IS, Barroilhet LM, Fu S, McHale MT, Schilder RJ, Farkkila A, Chowdhury D, Curtis J, Quinn RS, Bowes B, D'Andrea AD, Shapiro GI and Matulonis UA. Berzosertib plus gemcitabine versus gemcitabine alone in platinum-resistant high-grade serous ovarian cancer: a multicentre, open-label, randomised, phase 2 trial. Lancet Oncol 2020; 21: 957-968.
[48] Patil PD, Shapiro M, Hashemi Sadraei N and Pennell NA. An open-label phase II trial of bevacizumab plus docetaxel and gemcitabine in advanced, previously untreated nonsquamous non-small cell lung cancer. Oncologist 2019; 24: 457-e126.
[49] Ma T, Bai X, Wei Q, Shui Y, Lao M, Chen W, Huang B, Que R, Gao S, Zhang Y, Chen W, Wang J and Liang T. Adjuvant therapy with gemcitabine and stereotactic body radiation therapy versus gemcitabine alone for resected stage II pancreatic cancer: a prospective, randomized, open-label, single center trial. BMC Cancer 2022; 22: 865.
[50] Veldhuijzen van Zanten SEM, El-Khouly FE, Jansen MHA, Bakker DP, Sanchez Aliaga E, Haasbeek CJA, Wolf NI, Zwaan CM, Vandertop WP, van Vuurden DG and Kaspers GJL. A phase I/II study of gemcitabine during radiotherapy in children with newly diagnosed diffuse intrinsic pontine glioma. J Neurooncol 2017; 135: 307-315.
[51] Kim MM, Camelo-Piragua S, Schipper M, Tao Y, Normolle D, Junck L, Mammoser A, Betz BL, Cao Y, Kim CJ, Heth J, Sagher O, Lawrence TS and Tsien CI. Gemcitabine plus radiation therapy for high-grade glioma: long-term results of a phase 1 dose-escalation study. Int J Radiat Oncol Biol Phys 2016; 94: 305-311.
[52] Miwatashi S, Arikawa Y, Kotani E, Miyamoto M, Naruo K, Kimura H, Tanaka T, Asahi S and Ohkawa S. Novel inhibitor of p38 MAP kinase as an anti-TNF-alpha drug: discovery of N-[4-[2-ethyl-4-(3-methylphenyl)-1,3-thiazol-5-yl]-2-pyridyl]benzamide (TAK-715) as a potent and orally active anti-rheumatoid arthritis agent. J Med Chem 2005; 48: 5966-5979.
[53] Kudaravalli S, den Hollander P and Mani SA. Role of p38 MAP kinase in cancer stem cells and metastasis. Oncogene 2022; 41: 3177-3185.